Effect of chattering collisions on the self-diffusion coefficient of a dilute gas composed of infinitely thin hard needles

2001 J. Phys. A: Math. Gen. 34 4053

(http://iopscience.iop.org/0305-4470/34/19/307)

INSTITUTE OF PHYSICS PUBLISHING JOURNAL OF PHYSICS A: MATHEMATICAL AND GENERAL

J. Phys. A: Math. Gen. **34** (2001) 4053–4064 www.iop.org/Journals/ja PII: S0305-4470(01)21156-1

Effect of chattering collisions on the self-diffusion coefficient of a dilute gas composed of infinitely thin hard needles

Yosuke Yoshimura and Ayako Mukôyama

Department of Chemistry, Faculty of Science, Kyoto University, Kyoto 606-8502, Japan

E-mail: yyosuke@kuchem.kyoto-u.ac.jp

Received 15 January 2001

Abstract

The self-diffusion coefficient of a dilute gas composed of infinitely thin hard needles was studied by classical trajectory calculations in relation to the moment of inertia of the needle, I. The calculated self-diffusion coefficient was compared with the value obtained by the independent collision approximation (ICA) in which each collision is assumed to be uncorrelated. Both the self-diffusion coefficient and the collision frequency increase with decreasing moment of inertia of the needle as expected by the ICA. The increasing rate of the self-diffusion coefficient was proportional to $I^{-0.83}$ at $I \to 0$, that is larger than $I^{-1/2}$ by the ICA. However, the ICA gives a larger self-diffusion coefficient at large moment of inertia; the correlation between the impulses during the chattering collisions changes its sign from positive to negative with decreasing moment of inertia. The thermal rotational motion at the initial configuration reduces the effect of the collision-induced rotational motion that leads to the positive correlation. The rapid thermal rotational motion at small moment of inertia makes the chattering collisions a kind of reciprocating motion in the orientation of the needles.

PACS numbers: 05209D, 5110

1. Introduction

The transport coefficients of a dilute gas composed of hard spheres are evaluated exactly by the classical gas kinetic theory [1,2]. However, if the particle has a non-spherical shape, analytical evaluation of the transport coefficient will be unfeasible due to the chattering collisions [3]; a single scattering process between non-spherical particles can be composed of two or more collisions, which are called the chattering collisions. The chattering collisions bring about some correlation between the collisions even in dilute gases, and the independent collision approximation (ICA), which has sometimes been termed 'Enskog theory' [4], will not work well in evaluating the transport coefficients.

0305-4470/01/194053+12$30.00

The infinitely thin hard needle is the simplest model for a non-spherical hard body and their assembly gives the ideal gas at any densities [4]. The chattering collisions also take place between infinitely thin needles. They amount to 32% of all the collisions in the dilute gas composed of homogeneous needles and can continue more than a hundred times [5]. The molecular dynamics simulation, however, showed that the self-diffusion coefficient of the fluid composed of the homogeneous needles agreed well with the estimation by the ICA at low densities, although sizable deviation was found in the relaxation of the rotational energy [4]. The correlation among the chattering collisions is apparently extinguished in the self-diffusion coefficient for the homogeneous needle. The rate of the chattering collisions increases with the decrease in the moment of inertia by changing the mass distribution in the needle. We will demonstrate the effect of the chattering collisions on the self-diffusion coefficient over a wide range of moments of inertia of the needle I by classical trajectory calculations.

The ICA gives the correct self-diffusion coefficient at infinitely large moment of inertia where no chattering collisions occur. The trajectory calculations showed that the self-diffusion coefficient by the ICA deviates positively at large moment of inertia and negatively at small moment of inertia. The ICA is valid for a homogeneous needle that has the moment of inertia near the transition region between the positive and negative deviation. The deviation of the ICA indicates that the correlation between the impulses in the chattering collisions changes its sign with decreasing moment of inertia: a needle receives impulses from a similar direction during the chattering collisions, when the moment of inertia is large enough. Decreasing the moment of inertia, the motion of the needle during the chattering collisions becomes a kind of reciprocating motion with alternating orientation. The chattering collisions at small moment of inertia lead to the asymptotic dependence of the self-diffusion coefficient on the moment of inertia $\propto I^{-0.83}$ that is larger than the dependence by the ICA $\propto I^{-1/2}$. The trajectory calculation for non-rotating needles at the initial configuration showed that the rotational motion induced by the molecular collision plays a key role in the positive correlation. The rapid thermal rotational motion at small moment of inertia screens off the effect of the collision-induced rotational motion and brings about the negative correlation between the impulses during the chattering collisions.

This paper consists of six sections. The model is described in section 2 and several rigorous relations and the ICA are discussed in section 3. The computational procedure of the trajectory calculations is described in section 4, and the results of the trajectory calculations are given and discussed in section 5. The conclusions are given in section 6.

2. Model

Suppose we have a dilute gas composed of infinitely thin hard needles. The needle is assumed to be smooth, i.e. the impulse at the collision between two needles is perpendicular to both of the needles. For the sake of simplicity, we shall use the reduced units in which the length and the mass of the needle are unity. The temperature multiplied by the Boltzmann constant, $k_{\mathrm{B}}T$, is also set equal to unity to avoid the evident temperature dependence; e.g. the self-diffusion coefficient is proportional to $(k_{\mathrm{B}}T)^{1/2}$ at constant volume.

We consider a symmetrical needle in which the centre of mass coincides the centre of the needle. If the distribution of mass is limited within the needle length, the moment of inertia around the centre of mass I cannot exceed $1/4$. We, however, will consider the moment of inertia more than $1/4$ to demonstrate the effect of a large moment of inertia. No principles of motion are violated by assuming the needle of $I > 1/4$, although the mass distribution spreads out of the needle length. The needle rotates with the angular velocity ω. The orientation of the needle represented by the unit vector $\boldsymbol{u}$ is also given by ω and the phase of the rotational motion ψ.

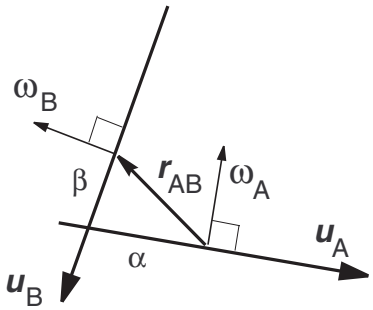

Figure 1. Configuration of needles A and B at collision.

The kinetic energy of a pair of needles A and B except for the energy relevant to the motion of the centre of mass, E_r, is expressed as

$$E_r = \tfrac{1}{4} v_r{}^2 + \tfrac{1}{2} I(\omega_A{}^2 + \omega_B{}^2). \tag{1}$$

The relative velocity $\boldsymbol{v}_r$ and the angular velocity of each needle obey the three- and the two-dimensional Maxwell–Boltzmann distribution, respectively. When two needles A and B collide, the following equations hold at the collision instant [4] (see figure 1):

$$(\boldsymbol{u}_A \times \boldsymbol{u}_B) \cdot \boldsymbol{r}_{AB} = 0 \tag{2}$$

$$|\alpha| < 0.5 \qquad |\beta| < 0.5 \tag{3}$$

where α and β in equation (3) represent the collision point along $\boldsymbol{u}$ of the needle A and B, respectively. Equation (2) indicates that two needles and the relative positional vector $\boldsymbol{r}_{AB}$ between A and B are in plane at the collision instant, and equation (3) restricts the collision point to the needle. The collision instant for a given initial condition at time $t = 0$ is determined by choosing the positive and the smallest root of equations (2) and (3), if the solution exists. The impulse at the collision instant $\Delta \boldsymbol{P}$ is given as

$$\Delta \boldsymbol{P} = -\frac{\boldsymbol{v}_{col}^{\perp}}{1 + (\alpha^2 + \beta^2)/(2I)} \tag{4}$$

where $\boldsymbol{v}_{col}$ is the relative velocity at the contact position

$$\boldsymbol{v}_{col} = \boldsymbol{v}_r + \beta(\omega_B \times \boldsymbol{u}_B) - \alpha(\omega_A \times \boldsymbol{u}_A) \tag{5}$$

and the superscript $\perp$ denotes the component perpendicular to the plane made by $\boldsymbol{u}_A$ and $\boldsymbol{u}_B$. The nth impulse in the chattering collisions is represented by $\Delta \boldsymbol{P}_n$.

3. Several rigorous results and the independent collision approximation

3.1. Independent collision approximation

We will define the collision as an event in which an impulse happens between the needles, and the scattering as a whole process in which the separate needles encounter one another and leave. A scattering is not necessarily composed of one collision. When a scattering contains two or more collisions, the collisions are termed the chattering collisions.

The mean collision frequency of a needle f_{col} is exactly evaluated by assuming the validity of the ergodicity. The collision frequency between two needles at a contact configuration is proportional to the number density ρ, the relative velocity at the contact position $v_{col}^{\perp}$, and the infinitesimal area around the contact point $|\boldsymbol{u}_A \times \boldsymbol{u}_B|\, d\alpha\, d\beta$. The total collision frequency is given as

$$f_{col} = \rho \int_{v_{col}^{\perp} > 0} v_{col}^{\perp}\, p(\boldsymbol{v}_{col}^{\perp}) \sin^2\theta\, d\theta\, d\alpha\, d\beta\, d\boldsymbol{v}_{col} \tag{6}$$

where θ is the angle between $\boldsymbol{u}_{\mathrm{A}}$ and $\boldsymbol{u}_{\mathrm{B}}$, and $p(\boldsymbol{v}_{\mathrm{col}}^{\perp})$ is the probability of finding $\boldsymbol{v}_{\mathrm{col}}^{\perp}$. The probability $p(\boldsymbol{v}_{\mathrm{col}}^{\perp})$ is a three-dimensional Maxwell–Boltzmann distribution for $\boldsymbol{v}_{\mathrm{r}}^{\perp}$, $(\omega_{\mathrm{B}} \times \boldsymbol{u}_{\mathrm{B}})^{\perp}$ and $(\omega_{\mathrm{A}} \times \boldsymbol{u}_{A})^{\perp}$. The explicit expression for the mean collision frequency is given as [4]

$$f_{\mathrm{col}} = \tfrac{8}{3}\pi^{1/2}\rho I F_{3/2}(8I) \tag{7}$$

where the function $F_n(x)$ is defined as

$$F_n(x) = \int_0^{\pi/4} \left[\left(1 + \frac{1}{x\cos^2\phi} \right)^n - 1 \right] \mathrm{d}\phi. \tag{8}$$

The integral in equation (8) is apparently expressed for $n = 1/2$ and $3/2$ as

$$F_{1/2}(x) = \frac{1}{\sqrt{x}} \ln \frac{\sqrt{x+2}+1}{\sqrt{x+1}} - \arccos\sqrt{\frac{x}{2(x+1)}} + \frac{\pi}{4} \tag{9}$$

$$F_{3/2}(x) = \frac{1}{2x\sqrt{x}} \left[\sqrt{x+2} + (x+1)\ln\frac{\sqrt{x+2}+1}{\sqrt{x+1}} \right] + F_{1/2}(x). \tag{10}$$

Equation (7) agreed fairly well with the results by the molecular dynamics simulation [4], because the collision frequency is fully determined by the velocity distribution at each collision instant. The transport coefficients, however, are dependent on the time correlation between the collisions. The effect of the time correlation between the collisions can be found even in the spherical molecules, because the scattered molecules will fall in a different macroscopic condition due to the non-uniform environment. The time correlation between the successive collisions after a long period compared with the time for the molecular interaction can be given by the systematic expansion of the distribution function with Sonine polynomials [1, 6]. We will neglect the higher-order approximation of the self-diffusion coefficient in the expansion by the Sonine polynomials throughout this paper.

The self-diffusion coefficient is evaluated by the scattering of the momentum, which corresponds to the relaxation of the velocity autocorrelation function. The first approximation of the self-diffusion coefficient in the expansion by Sonine polynomials is given as

$$1/D = -\frac{I^2}{128\pi^{11/2}} \frac{\rho}{3} \int [\boldsymbol{v}_{\mathrm{r}} \Delta \boldsymbol{v}_{\mathrm{r}}] v_{\mathrm{r}} \exp(-E_{\mathrm{r}})\, \mathrm{d}\sigma\, \mathrm{d}\boldsymbol{v}_{\mathrm{r}}\, \mathrm{d}\omega_{\mathrm{A}}\, \mathrm{d}\omega_{\mathrm{B}}\, \mathrm{d}\psi_{\mathrm{A}}\, \mathrm{d}\psi_{\mathrm{B}} \tag{11}$$

$$= \rho \tfrac{2}{3} \langle\langle (\Delta \boldsymbol{P})^2 \rangle\rangle \tag{12}$$

where $\Delta \boldsymbol{v}_{\mathrm{r}}$ is the change of the relative velocity in the whole scattering process and σ is the differential cross section. $\rho\langle\langle X \rangle\rangle$ represents the mean value of X for a single needle scattered in the unit time; for example, the scattering frequency f_{scat} is expressed as $\rho\langle\langle 1 \rangle\rangle$.

If the scattering is composed of many collisions, the change of the impulse $\Delta \boldsymbol{P}$ in equation (11) is evaluated by the sum of the impulses $\Delta \boldsymbol{P}_n$. The square of the impulse during the whole scattering process is expressed as

$$\langle\langle (\Delta \boldsymbol{P})^2 \rangle\rangle = \sum_i \langle\langle (\Delta \boldsymbol{P}_i)^2 \rangle\rangle + 2 \sum_i \sum_{n>0} \langle\langle \Delta \boldsymbol{P}_i \Delta \boldsymbol{P}_{i+n} \rangle\rangle \tag{13}$$

$$= S(0) + \sum_{n>0} S(n) \tag{14}$$

where $S(n)$ is the term relevant to the correlation with the impulse at the nth collision counted from each collision. If the successive collisions are uncorrelated, the self-diffusion coefficient can be evaluated from the information on the single collision $S(0)$ as in the case of the collision frequency. The integral can be carried out as [4]

$$1/D = \tfrac{16}{3}\pi^{1/2}\rho I F_{1/2}(8I). \tag{15}$$

We shall call the approximation the ICA.

3.2. Asymptotic behaviour at small and large moment of inertia

The asymptotic expressions of the function $F_n(x)$ at $x \to 0$ and $x \to \infty$ are given as

$$F_n(x) = \begin{cases} C_n/x^n & x \to 0 \\ n/x & x \to \infty \end{cases} \tag{16}$$

where $C_{1/2} = \ln(2^{1/2}+1)$ and $C_{3/2} = 2^{-1/2} + (1/2)\ln(1+2^{1/2})$. The collision frequency and the self-diffusion coefficient given by the ICA converge at a finite value with increasing the moment of inertia and diverge in proportion to $I^{-1/2}$ with $I \to 0$.

The collision frequency given in equation (7) diverges with the decrease in the moment of inertia in proportion to $I^{-1/2}$, because the relative velocity at the contact position v_{col} increases with increasing the mean angular velocity as $I^{-1/2}$. The scattering frequency, however, is finite even at the limit of $I = 0$. The total scattering cross section between needles σ_{total} at $I \to 0$ is equivalent to the cross section between hard discs without the rotation along the in-plane axis given as (see the appendix)

$$\sigma_{\mathrm{total}}(I \to 0) = \frac{\pi^3}{32} + \frac{\pi}{4}. \tag{17}$$

The infinite collision frequency and the finite scattering frequency at $I \to 0$ indicate that the chattering collisions are predominant at small moment of inertia.

The self-diffusion coefficient will also diverge with decreasing moment of inertia, although the scattering frequency is finite when $I \to 0$. The self-diffusion coefficient is qualitatively expressed by the mean free path λ and the mean velocity $\langle v_{\mathrm{r}} \rangle$ as [1, 2]

$$D \propto \frac{1}{1-R_{\mathrm{p}}} \lambda \langle v_{\mathrm{r}} \rangle \tag{18}$$

where R_{p} is the persistence of the translational velocity at the collision and the mean free path λ is defined as $\langle v_{\mathrm{r}} \rangle / f_{\mathrm{scat}}$ or $\langle v_{\mathrm{r}} \rangle / f_{\mathrm{col}}$ depending on the context. The persistence of the translational velocity is the ratio of the translational velocity after the collision in the same direction as the velocity before the collision [2]; the fatigability $1 - R_{\mathrm{p}}$ is the mean ratio of the impulse along the incident velocity $\Delta P^{\parallel}$ to the incident velocity v_{in} as $\langle -\Delta P^{\parallel}/v_{\mathrm{in}} \rangle$. The impulse at each collision decreases almost in proportion to I with $I \to 0$ as shown in equation (4). The asymptotic expression of the ICA (see equations (15) and (16)) indicates that the self-diffusion coefficient diverges with $I \to 0$ by the larger decreasing rate in the fatigability of the velocity ($\propto I$) than that in the mean free path ($\langle v_{\mathrm{r}} \rangle / f_{\mathrm{col}} \propto I^{1/2}$). The correct self-diffusion coefficient may have the same dependence on the moment of inertia as the ICA, if the correlation among the chattering collisions does not depend strongly on the moment of inertia; the fatigability for a whole scattering will decrease in proportion to $I^{1/2}$, because the number of collisions in a single scattering $f_{\mathrm{col}}/f_{\mathrm{scat}}$ increases in proportion to $I^{-1/2}$ with decreasing moment of inertia.

When the moment of inertia is infinitely large, the hard needle will not rotate in a finite time. The ICA gives the correct results at $I \to \infty$, because the chattering collisions will not happen. The total cross section σ_{total} of the scattering (collision) between non-rotating needles is given as (see the appendix):

$$\sigma_{\mathrm{total}}(I \to \infty) = \frac{\pi}{8} \tag{19}$$

which is identical to the limiting expression of the scattering (collision) frequency $\langle v_{\mathrm{r}} \rangle \sigma_{\mathrm{total}}$ at $I \to \infty$ by equation (7)

$$f_{\mathrm{scat}}(I \to \infty) = \frac{\pi^{1/2}}{2}. \tag{20}$$

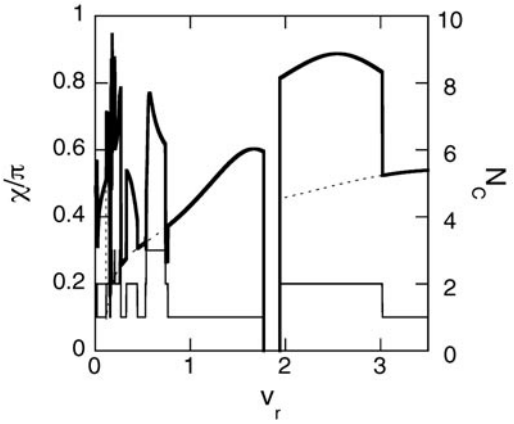

Figure 2. Change of the scattering angle χ (thick solid line) and the collision number N_C (thin solid line) with the incident relative velocity v_r for a pair of homogeneous needles $I = 1/12$. The dotted line represents the scattering angle at the first collision χ_1. The impact parameter b is 0.3 and the initial rotational condition of each needle is given as ($\omega = 3.0, \theta = 0.5\pi, \phi = -0.5\pi, \psi = 0.1\pi$) and ($\omega = 5.0, \theta = 0.2\pi, \phi = 0.3\pi, \psi = 0.5\pi$), where θ and ϕ are the polar angles of the angular velocity.

4. Computational procedure

The integration on the scattering process was carried out by the classical trajectory calculation with a Monte Carlo technique. We generated 1×10^6 configurations of a needle pair at the unit distance for a given value of the moment of inertia. The needles were separated by unit distance and move along the same axis. The orientation of each needle was generated isotropically, and the impact parameter b in each trial was sampled with the statistical weight proportional to b. The relative translational velocity and the angular velocity were generated as they satisfy the three- and the two-dimensional Maxwell–Boltzmann distribution, respectively.

Equation (2) was solved numerically by the same algorithm as described in [5], that is the combination of the second-order Newton–Raphson method [4] and the time evolution with a constant time step evaluated by the angular velocities of the needles. We confirmed that the distribution of the relative translational velocity and the angular velocity does not change with the scattering, i.e. the Maxwell–Boltzmann distribution is a stationary distribution. The moment of inertia was changed from 1 to 10^{-4}. We also carried out the trajectory calculation for the non-rotating needles ($\omega = 0$) at the initial configuration to elucidate the effect of the thermal rotational motion.

5. Results and discussions

5.1. Scattering and collision frequencies

Trajectories of needles change in a discontinuous manner with continuous change in the initial conditions. A typical example is shown for the scattering angle χ in figure 2. The curve of the scattering angle against the incident relative velocity is piecewise smooth. The segmentation of the scattering angle is principally due to the non-analytic conditions in determining the collision instance between needles (equation (3) and the time order of the solutions): e.g. when the collision point departs from the end of either needle with the change in the relative velocity, new configuration of collision becomes apparent. The segmentation in a single collision with the continuous change in the relative velocity is shown in the scattering angle at the first collision χ_1 in figure 1. No available configuration of collision is found for the relative velocity between 1.78 and 1.93. The segmentation in a single collision is enhanced by the successive collisions, i.e. the chattering collisions. Since the segmentation in a single collision also holds in each collision in the chattering collisions, the scattering process becomes too complicated to describe in an explicit manner.

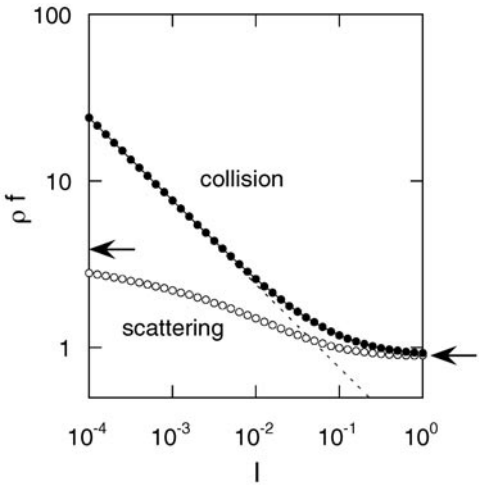

Figure 3. Change in the scattering (○) and the collision (●) frequencies with the moment of inertia of the needle. The solid curve represents the analytical result for the collision frequency by equation (7), and the dotted curve represents the asymptotic expression by equation (16). The arrows denote the limiting scattering frequency at $I \to 0$ and $I \to \infty$.

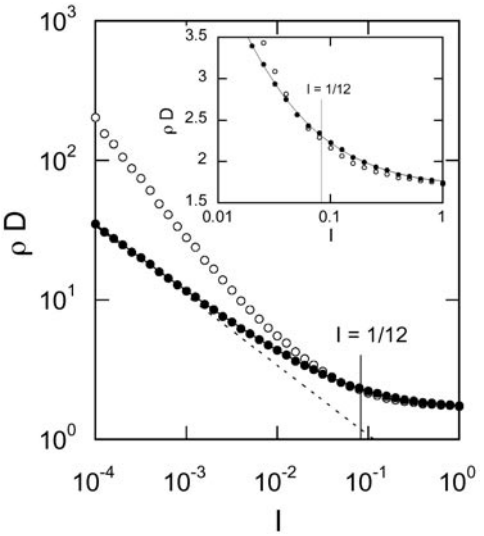

Figure 4. Dependence of the self-diffusion coefficient (○) on the moment of inertia of the needle by the trajectory calculation. The ICA (●) gives smaller self-diffusion coefficient at $I < 0.047$. The solid curve represents the analytical result by the ICA (equation (15)), and the dotted curve represents the asymptotic expression by equation (16). The inset shows the region where the sign of the deviation is changed.

Despite the complexity in the trajectories, the ergodic characteristic of the system gives an exact result on the collision frequency as in equation (7). The calculated scattering and collision frequencies are shown in figure 3. The excellent agreement in the collision frequency with equation (7) confirms the ergodicity of the system. Both the scattering and the collision frequencies increase with decreasing moment of inertia. The collision frequency increases almost in proportion to $I^{-1/2}$ at $I < 0.01$ as shown in equation (16). The scattering frequency slowly converges at a limiting value given by equation (17) with $I \to 0$. The ratio of $f_{\mathrm{col}}/f_{\mathrm{scat}}$, i.e. the average collision number in a scattering process, increases with decreasing moment of inertia from 1.03 at $I = 1$ to 3.46 at $I = 0.001$. The average collision number in a single scattering exceeds two at $I < 0.0055$.

5.2. Self-diffusion coefficient

The effect of the moment of inertia on the self-diffusion coefficient is shown in figure 4. The value of the ICA by the trajectory calculation agreed fairly well with the analytical result in equation (15). The self-diffusion coefficient increases with decreasing moment of inertia, as discussed in section 3.2. The contribution from the decrease in the fatigability of the velocity at each collision ($\propto I$) exceeds that from the increase in the collision frequency ($\propto I^{-1/2}$). The increasing rate of the self-diffusion coefficient, however, is almost proportional to $I^{-0.83}$ at $I < 0.001$. The correlation in the chattering collisions works efficiently in decreasing the fatigability of the whole scattering process and leads to an extra factor proportional to $I^{0.33}$ at small moment of inertia.

The ICA is correct at infinitely large moment of inertia, where no chattering collisions

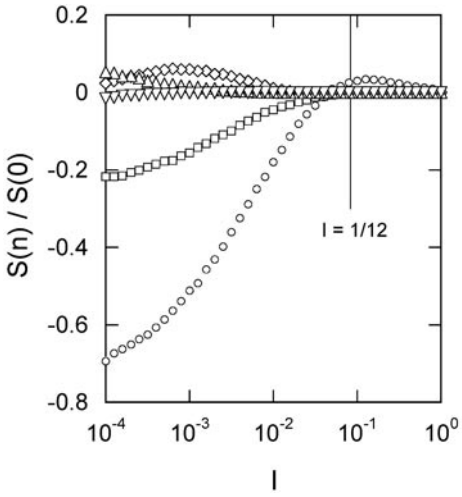

Figure 5. Change in the correlation terms between the impulses in the chattering collisions $S(n)$ with the moment of inertia of the needle. ○, $n = 1$; □, $n = 2$; ◇, $n = 3$; △, $n = 4$; ▽, $n = 5$.

happen. The ICA gives slightly larger self-diffusion coefficient at large moment of inertia, and the deviation changes its sign from positive to negative around $I = 0.047$ and increases with decreasing moment of inertia. The terms relevant to the correlation among the impulses in equation (14) have a different sign at large and small moment of inertia. The ICA works well for large moment of inertia and for the moment of inertia around $I = 0.047$; the ICA was successful for the self-diffusion coefficient in the low-density fluid of the homogeneous needle [4], the moment of inertia of which, $I = 1/12$, is near $I = 0.047$.

5.3. Correlation among the impulses during the chattering collisions

The correlation in the chattering collisions changes the asymptotic characteristics of the self-diffusion coefficient at $I \to 0$ and it gives positive or negative deviation of the ICA depending on the moment of inertia as shown in section 5.2. The effect of the chattering collisions arises mainly from the correlation with the adjacent and the second-adjacent collisions. The correlation terms between the impulses in the chattering collisions in equation (14) are shown in figure 5. The contributions from the correlation terms $S(n > 0)$ are damped rapidly with increasing number of intermediate collisions. The correlation term with the adjacent collision $S(1)$ explains more than 80% of the deviation of the ICA in figure 4, except for the region around $I = 0.047$, where the correlation terms are very small.

The correlation terms with separated collisions are small, but contribute to the resulting self-diffusion coefficient at small moment of inertia. The correlation terms relevant to the adjacent and the second-adjacent collisions $S(1)$ and $S(2)$ reduce the value of the ICA to one-third $[S(1) + S(2)]/S(0) = -0.67$ at $I = 0.001$. Although the total amount of the correlation terms relevant to the separated collisions $S(n > 2)$ is $+0.079S(0)$ at $I = 0.001$, it accounts for 19% of the resulting self-diffusion coefficient. The contribution from the correlation terms with the separated collisions increases with decrease in the moment of inertia: the sum of the correlation terms $S(n > 2)$ at $I = 0.0001$ is $+0.083S(0)$, that is not very different from the value at $I = 0.001$. However, its ratio in the resulting self-diffusion coefficient is 48%, because the correlation terms $S(1)$ and $S(2)$ amount to $-0.91S(0)$ at $I = 0.0001$. We cannot neglect the correlation between separated collisions in considering the asymptotic behaviour of the self-diffusion coefficient at small moment of inertia.

The correlation between the impulses in figure 5 suggests that different mechanisms work

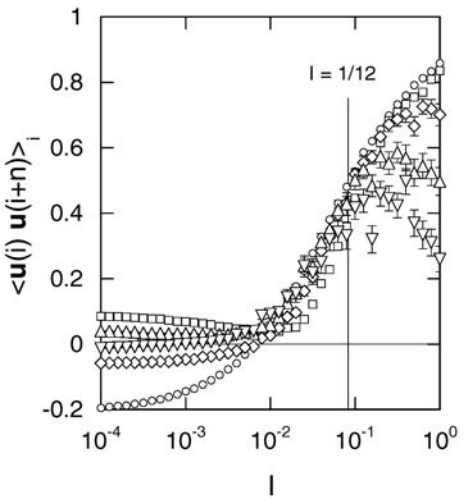

Figure 6. Change in the correlation between the needle orientation $\langle \boldsymbol{u}(i)\boldsymbol{u}(i+n)\rangle_i$ during the chattering collisions with the moment of inertia of the needle. ○, $n = 1$; □, $n = 2$; ◇, $n = 3$; △, $n = 4$; ▽, $n = 5$. The error bars indicate the standard deviation.

at large and small moment of inertia. When the moment of inertia is large enough, the chattering collisions will happen between slightly rotating needles, i.e. the configuration of the needle pair is not very different for adjacent collision; the impulses in the chattering collisions will come from a similar direction, which leads to the positive correlation. On the other hand, when the moment of inertia is small, the orientation of the needles can change drastically with adjacent collision; for example, a needle will hit its counterpart on another wing from the opposite side in successive collisions.

The change in the orientation of the needle during the chattering collisions can be evaluated by the scalar product of the orientation vector $\boldsymbol{u}(i)$ at the ith collision with that at the successive collisions. Figure 6 shows the orientational correlation with the nth collision counted from the ith collision in the chattering collisions $\langle \boldsymbol{u}(i)\boldsymbol{u}(i+n)\rangle_i$, where $\langle X\rangle_i$ denotes the average over all the ith collisions in the chattering collisions. The rotating angle between the adjacent collisions increases with decrease in the moment of inertia, and the rotating angle will exceed a right angle at around $I = 0.007$ on average.

The orientational correlation in figure 6 shows that the chattering collisions have different characteristics in the following three regions: (i) $I > 0.1$, (ii) $0.01 < I < 0.1$ and (iii) $I < 0.01$. The rotational angle during the chattering collisions increases monotonically with increase in the intermediate collisions at $I > 0.1$; the needle moves almost on a plane in a certain direction during the chattering collisions at $I > 0.1$. The motion will be confined on a conical surface at $0.01 < I < 0.1$ where the rotational angles between successive collisions are not very different; $\langle \boldsymbol{u}(i)\boldsymbol{u}(i+n)\rangle_i$ for the homogeneous needle ($I = 1/12$) is 0.49, 0.38 and 0.44 at $n = 1, 2, 3$, respectively. Decreasing further the moment of inertia, the orientation of the needle changes in an oscillatory manner at $I < 0.01$; the sign of the orientational correlation changes alternately with the number of intermediate collisions. The alternating behaviour at $I < 0.01$ is also found in the correlation in the collision point; the correlation between the collision point $\langle \alpha(i)\alpha(i+n)\rangle_i$ at $I = 0.001$ was 0.102, -0.023, 0.005 and -0.003 for $n = 0, 1, 2, 3$, respectively.

5.4. Importance of the thermal rotational motion in the chattering collisions

The thermal rotational motion of the needles will be responsible for the different characteristics of the chattering collisions in a wide range of the moment of inertia as shown in the preceding

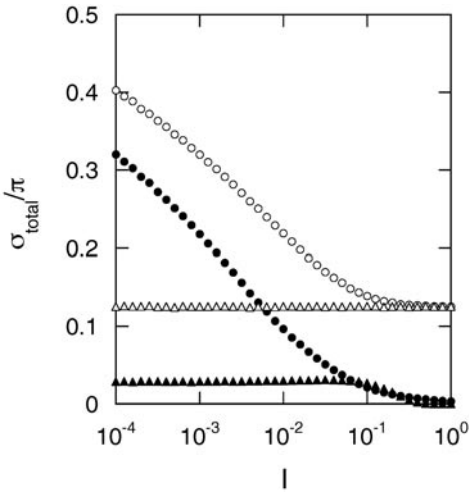

Figure 7. Total scattering cross sections between the thermally rotating needles (○) and between the non-rotating needles (△) at the relative velocity $v_r = 4/\pi^{1/2}$. Closed symbols represent the cross section of the scattering followed by the chattering collisions. The limiting cross section between the thermally rotating needles at $I \to 0$ in equation (17) is out of the pane (0.5584π).

sections. We carried out the trajectory calculations at a fixed relative translational velocity for the non-rotating needles and the thermally rotating needles at the initial configuration. The initial relative velocity was fixed at the thermal mean velocity $4/\pi^{1/2}$.

Figure 7 shows the effect of the thermal rotational motion on the scattering cross section. The total scattering cross section σ_{total} between non-rotating needles ($\omega_{t=0} = 0$) is constant at $\pi/8$ as shown in equation (19), while σ_{total} between thermally rotating needles increases with decreasing moment of inertia to the limiting value in equation (17). The scattering cross section followed by the chattering collisions between non-rotating needles becomes apparent at $I < 0.5$, and it is almost constant for $I < 0.1$ with a small maximum 0.031π around $I = 0.03$. The chattering collisions between the non-rotating needles were not detected in the present calculations at $I > 0.8$. The thermally rotating needles have much larger cross section followed by the chattering collisions at small moment of inertia. The thermal rotational motion will play an essential role in the chattering collisions.

Figure 8 shows the change in the square of the total impulse during the scattering process together with the values by the ICA. The results for the thermally rotating needles at fixed relative velocity agree well with those found in the self-diffusion coefficient in figure 4; the square of the total impulse is larger than the value by the ICA at large moment of inertia ($I > 0.06$) and gives the same asymptotic dependence on the moment of inertia at small moment of inertia ($\propto I^{0.83}$). The thermal distribution of the relative velocity is not responsible for the qualitative characteristics of the self-diffusion coefficient in figure 4. The square of the total impulse between the non-rotating needles is proportional to I at $I \to 0$:

$$\langle(\Delta \boldsymbol{P}(I \to 0))^2\rangle \propto \int_0^\infty \frac{\mathrm{d}\alpha\,\mathrm{d}\beta}{[1 + (\alpha^2 + \beta^2)/(2I)]^2} \propto I. \tag{21}$$

The decreasing rate of the square of the total impulse between the thermally rotating needles ($\propto I^{0.83}$) is between those by the ICA ($\propto I^{1/2}$) and the result for the non-rotating needles ($\propto I$).

The ICA always gives a smaller value for the square of the total impulse between the non-rotating needles, i.e. the correlation terms are positive irrespective of the moment of inertia. The alternation in the orientational correlation at small moment of inertia in figure 6 was not found in the scattering between the non-rotating needles either. The negative correlation between the impulses at small moment of inertia is attributed to the thermal rotational motion of the needles.

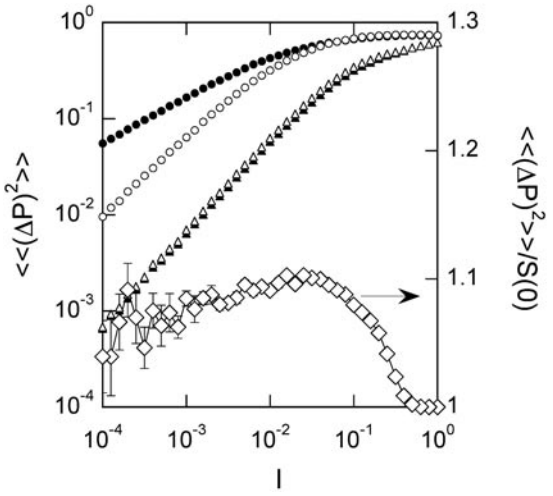

Figure 8. Change of the square of the total impulse during the scattering process $\langle\langle(\Delta \boldsymbol{P})^2\rangle\rangle$ for the thermally rotating needles (○) and the non-rotating needles (△) at the relative velocity $v_r = 4/\pi^{1/2}$. Closed symbols represent the value by the ICA $S(0)$. The ratio of the square of the total impulse to the value by the ICA is shown for the non-rotating needle by ◇. The error bars indicate the standard deviation.

6. Conclusions

The self-diffusion coefficient of a dilute gas composed of infinitely thin hard needles is overestimated at large moment of inertia and underestimated at small moment of inertia by the ICA: the correlation between the impulses during the chattering collisions changes from positive to negative at $I > 0.047$ with decreasing moment of inertia. The positive correlation between impulses is due to the chattering collisions accompanied by the collision-induced rotational motion. The thermal rotational motion reduces the effect of the collision-induced rotational motion and gives the negative correlation at small moment of inertia. The chattering collisions at small moment of inertia ($I < 0.01$) are governed by the rapid thermal rotational motion and they seem to be a reciprocating motion with alternating orientation of the needle. Since the chattering collisions at small I will bring about extra correlation between the impulses proportional to $I^{0.33}$, the self-diffusion coefficient has a larger dependence on the moment of inertia ($\propto I^{-0.83}$) than does that by the ICA ($\propto I^{-1/2}$). Although the contribution from the correlation with the adjacent and the second-adjacent collisions $S(1) + S(2)$ is dominant in the correlation terms, the correlation between the separated collisions cannot be neglected in determining the resulting self-diffusion coefficient at small moment of inertia, because the autocorrelation term $S(0)$ is reduced greatly by the correlation terms with the adjacent and the second-adjacent collisions $S(1) + S(2)$.

The effect of the chattering collisions on the transport coefficients is not evident even in the simplest system demonstrated here. The chattering collisions have different characteristics depending on the contribution from the collision-induced rotational motion, i.e. the energy transfer from translation to rotation. A detailed study on the rotational modes that lead to the chattering collisions is necessary to elucidate the role of the collision-induced and the thermal rotational motion in determining the correlation between the impulses in the chattering collisions. The knowledge of the rotational mode relevant to the chattering collisions will show us a simple and transparent picture on the different effects of the chattering collisions on the other transport coefficients such as the thermal conductivity [3].

Appendix. Total cross section at small and large moment of inertia

The total scattering cross section between needles at the limit of $I = 0$ is equivalent to the cross section between hard discs of diameter unity without rotation along the in-plane axis. The total cross section σ_{total} of the collision between non-rotating hard discs A and B is evaluated by using their projections on a plane; the projections C_{A} and C_{B} are the ellipse the major axis of which is unity. The total cross section is expressed as

$$\sigma_{\text{total}} = \frac{1}{2\pi}\left\langle \int_{C_{\text{A}}} \mathrm{d}C_{\text{B}} \right\rangle_{C_{\text{A}},C_{\text{B}}} \tag{A.1}$$

where the integral is taken over all the configurations in which the projections C_{A} and C_{B} are overlapped, and the integral is averaged over all the orientation of the hard discs A and B. The integral is evaluated as [7]

$$\sigma_{\text{total}} = \frac{1}{2\pi}\langle L_{\text{A}}\rangle_{C_{\text{A}}}\langle L_{\text{B}}\rangle_{C_{\text{B}}} + (\langle S_{\text{A}}\rangle_{C_{\text{A}}} + \langle S_{\text{B}}\rangle_{C_{\text{B}}}). \tag{A.2}$$

The mean length of the circumference and the mean area of the ellipse, $\langle L\rangle_C$ and $\langle S\rangle_C$, are calculated as $\pi^2/4$ and $\pi/8$, respectively, and we obtain equation (17).

When the moment of inertia is infinitely large, the hard needle will not rotate in a finite time. The chattering collisions will not happen in this limit, and the collision frequency is identical to the scattering frequency. The total cross section of the collision between the non-rotating needles is given by the same procedure as above with $\langle L\rangle_C = \pi/4$ and $\langle S\rangle_C = 0$, where C is the projection of the line of the unit length on a plane.

References

[1] Chapman S and Cowling T G 1970 *The Mathematical Theory of Non-Uniform Gases* 3rd edn (Cambridge: Cambridge University Press)
[2] Jeans J 1940 *An Introduction to the Kinetic Theory of Gases* (Cambridge: Cambridge University Press)
[3] Cole R G, Evans D R and Hoffman D K 1985 *J. Chem. Phys.* **82** 2061
[4] Frenkel D and Magnuire J F 1983 *Mol. Phys.* **49** 503
[5] Mukôyama A and Yoshimura Y 1997 *J. Phys. A: Math. Gen.* **A30** 6667
[6] Reichl L E 1998 *A Modern Course of Statistical Physics* 2nd edn (New York: Wiley–Interscience)
[7] Santaló L A 1952 *Actualites Sci. Indust.* **1198**